AD-A150 604 CLUSTERING AND ORDERING IN III-V ALLOYS(U) WASHINGTON 1/1
UNIV ST LOUIS MO SEMICONDUCTOR RESEARCH LAB
C M WOLFE ET AL. 31 JUL 84 WU/SRL-59583A-3
UNCLASSIFIED AFOSR-TR-84-1276 AFOSR-82-0231 F/G 11/6 NL

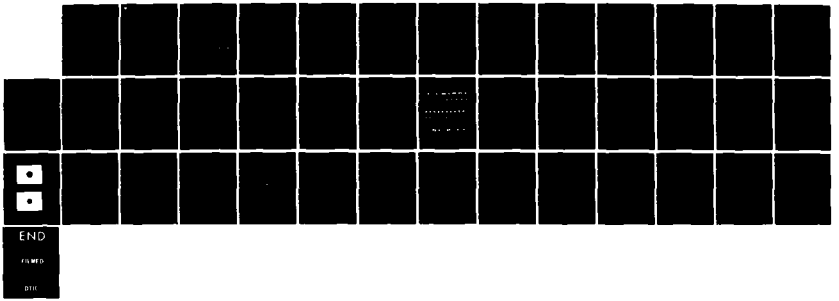

END
FILMED
DTIC

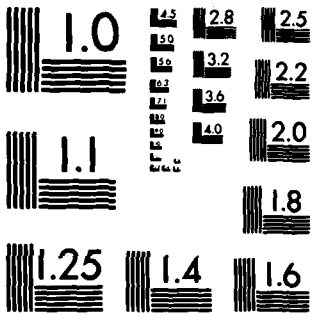

MICROCOPY RESOLUTION TEST CHART
NATIONAL BUREAU OF STANDARDS-1963-A

WASHINGTON UNIVERSITY IN ST. LOUIS

AFOSR-TR- 84-1276

CLUSTERING AND ORDERING IN III-V ALLOYS

SEMICONDUCTOR RESEARCH LABORATORY

Washington University

Saint Louis, Missouri 63130

31 July 1984

1 June 1983 to 31 May 1984

ANNUAL SCIENTIFIC REPORT NO. WU/SRL-59583A-3

Air Force Office of Scientific Research
Building 410
Bolling Air Force Base, DC20332

Grant No. AFOSR-82-0231

Unclassified

SECURITY CLASSIFICATION OF THIS PAGE (When Data Entered)

Capt Malloy

REPORT DOCUMENTATION PAGE	READ INSTRUCTIONS BEFORE COMPLETING FORM
1. REPORT NUMBER: AFOSR-TR- 84-1276 / 2. GOVT ACCESSION NO.: A150 604	3. RECIPIENT'S CATALOG NUMBER:
4. TITLE (and Subtitle): Clustering and Ordering in III-V Alloys	5. TYPE OF REPORT & PERIOD COVERED: Annual; 1 Jun 83 - 31 May 84
	6. PERFORMING ORG. REPORT NUMBER: WU/SRL-59583A-3
7. AUTHOR(s): C.M. Wolfe, M.W. Muller, P.A. Fedders, S. Julie Hsieh, Elizabeth A. Patten, K.A. Salzman	8. CONTRACT OR GRANT NUMBER(s): AFOSR-82-0231
9. PERFORMING ORGANIZATION NAME AND ADDRESS: Washington University, Box 1127, St. Louis, MO 63130	10. PROGRAM ELEMENT, PROJECT, TASK AREA & WORK UNIT NUMBERS: 61102F; 2306/B1
11. CONTROLLING OFFICE NAME AND ADDRESS: Air Force Office of Scientific Research, Building 410, Bolling AFB, DC 20332	12. REPORT DATE: 31 Jul 84 13. NUMBER OF PAGES: 37
14. MONITORING AGENCY NAME & ADDRESS (if different from Controlling Office)	15. SECURITY CLASS. (of this report): Unclassified 15a. DECLASSIFICATION/DOWNGRADING SCHEDULE

16. DISTRIBUTION STATEMENT (of this Report)

The United States Government is authorized to reproduce and distribute this report for Governmental purposes.

Approved for public release; distribution unlimited.

17. DISTRIBUTION STATEMENT (of the abstract entered in Block 20, if different from Report)

18. SUPPLEMENTARY NOTES

19. KEY WORDS (Continue on reverse side if necessary and identify by block number)

Alloy composition, fluctuations, ordering, $In_xGa_{1-x}P$, GaAs, $ZnSnP_2$, crystal structure, chalcopyrite, heterojunctions, interfacial energy gaps.

20. ABSTRACT (Continue on reverse side if necessary and identify by block number)

The III-V semiconducting alloys are typically grown by epitaxial techniques at temperatures where, in the absence of substrate effects, they are thermodynamically unstable. This can result in problems associated with clustering of like atoms or ordering of unlike atoms. Long-range ordering could yield interesting III-V ternary compounds.

The mixing enthalpy of III-V semiconductor alloys is fairly well described by regular solution theory, with a thermodynamic

DD FORM 1 JAN 73 1473 EDITION OF 1 NOV 65 IS OBSOLETE

Unclassified

SECURITY CLASSIFICATION OF THIS PAGE (When Data Entered)

20. Abstract (Continued)

interaction parameter that is sensitive to the lattice spacing of the binary constituents. An estimate of the interaction parameter is derived from a model which ascribes the mixing enthalpy to bond distortions associated with the alloy formation, and relates these to the macroscopic elastic properties of the crystal. Numerical estimates are given for the 18 alloys with cations Al, Ga, In and anions P, As, Sb, and these are compared with experimental values and alternative models. To within a single adjustable parameter, the predictions agree with experiment and are consistent with those of the delta lattice parameter (DLP) model. Originator Furnished

A calculation of the elastic energy associated with composition fluctuations (clustering) in these alloys indicates that this energy is sufficient to suppress clustering above the critical mixing temperature. For semiconductor alloys $A_xB_{1-x}C$ where the lattice parameters of AC and BC differ, clustering is reduced below that exhibited by a purely random distribution. This provides a tendency toward order in these alloys. The extent to which clustering is reduced is estimated and related to recent observations of Raman linewidths and lineshapes in $In_{1-x}Ga_xAs$ and $Al_{1-x}Ga_xAs$.

Below bandgap photovoltaic response with a half-power point at 1.31eV is observed in p-type $In_{1-x}Ga_xP$ on n-type GaAs heterojunctions with {111} interfaces. This response is apparently due to photon-assisted tunneling of carriers across the interfacial energy gap, which is smaller than the energy gaps of the constituent materials. The same mechanism can be employed in other heterojunctions with appropriate energy band lineups to obtain longer wavelength infrared response.

Keywords include:

(Field 19)

TABLE OF CONTENTS

1. INTRODUCTION

Although there is substantial interest in III-V semiconductor alloys for electronic and optoelectronic devices, relatively little is known about the distribution of atoms in these materials or the effects of non-random distributions on device performance. In many of these alloys, however, non-random distributions of atoms are expected to be important from thermodynamic considerations. This is particularly true at the low temperatures commonly used for epitaxial growth. The available evidence suggests that short-range clustering of like atoms or short-range ordering of unlike atoms can produce device problems such as excess noise and leakage current, premature voltage breakdown, and lower carrier mobilities. Long-range ordering of unlike atoms, however, could potentially yield III-V ternary compounds with properties superior to their parent alloys. In epitaxial growth, substrate effects such as lattice match and nonequivalent sublattice sites are expected to have a strong influence on these phenomena. Also, two of the important III-V alloys, $Ga_xIn_{1-x}P$ and $Ga_xIn_{1-x}As$, can be epitaxially grown lattice matched to GaAs and InP, respectively, at compositions near the point of greatest ordering probability. The objective of this work is to investigate various aspects of clustering and ordering in these materials.

2. ELASTIC MODEL OF III-V ALLOY FORMATION

The calculation of phase diagrams and of other thermodynamic properties of tetrahedral ternary III-V semiconductor alloys of the form $A_xB_{1-x}C$ (or AC_xD_{1-x}) using regular solution theory has proved to be a useful and reasonably accurate approximation. Several of the ternary alloys with cations Al, Ga, In and anions P, As, Sb have important present or potential applications in electronic technology. These eighteen alloys are mixtures of binary compounds with, in general, different lattice parameters. The lattice parameters of the binary compounds are different when the AC and BC bond lengths are different, and the lattice parameter of the alloy then differs from both. The lattice parameters of all the ternary alloys that can be formed from the ions listed except those involving the cation pair Al, Ga are sensitive to composition. One then may take the view that the bonds are distorted or rearranged in forming the alloy. The energy associated with the bond distortion can be estimated from the macroscopic elastic properties of the crystals. We discuss the contribution of this energy to the enthalpy of mixing and its effect on clustering and spinodal decomposition. We suggest that it is a major or dominant factor in both phenomena.

2.1 MIXING ENTHALPY

In regular solution theory the molar enthalpy of mixing of a binary solution is given by

$$\Delta H_m = x(1-x)\Omega \qquad (1)$$

where Ω is the interaction parameter and where x and 1 - x are the fractions of the components making up the solution. In terms of a picture of pairwise interaction energies, the interaction parameter is

$$\Omega = 6N_o\varepsilon \tag{2}$$

where $6N_o$ is the number of interacting pairs on the fcc sublattice and

$$\varepsilon = 2\varepsilon_{AB} - \varepsilon_{AA} - \varepsilon_{BB} \tag{3}$$

is the excess of the AA and BB bond energies between like ions over the AB bond energy of unlike ions. In the ternary alloys under discussion these second nearest neighbor interactions are thought to be rather small, consistent with the small experimental values of the interaction parameter.

Stringfellow, using the covalent bonding ideas of Phillips and Van Vechten[1], has introduced the delta lattice parameter model[2] which provides values of the interaction parameter of all the alloys in terms of a single adjustable parameter. The agreement between the DLP theory and experiment is remarkably good for a theory with a single adjustable parameter. The model takes a less specific approach than the identification of Equations (2) and (3) of the interaction parameter with the sum of binary bond energies, and assumes that the energy is a more global property of the semiconductor that depends only on the lattice parameter of the crystal. The idea is that the bonding energy is proportional to the band gap which, in turn,

is proportional to a power of the lattice parameter. This is similar to but distinct from Van Vechten's proposal[3] that Ω is produced by the reduction of the band gaps due to the disorder associated with alloying. The DLP model leads to an approximate value for Ω of

$$\Omega_s = (35/8)K\Delta^2\bar{d}^{-4.5} \tag{4}$$

where $\Delta = a - b$, $\bar{d} = 1/2(a+b)$, with a and b the lattice parameters of AC and BC, respectively. The quantity K is obtained by a least squares fit to the experimental data and is equal to 1.15×10^7 cal/mole $\text{Å}^{2.5}$. The excellent fit to the experimental data depends largely on the Δ^2 dependence of Ω.

We wish to show here that if part or all of Ω is interpreted as being associated with strain or lattice parameter mismatch, then it is readily shown that this contribution exhibits the same Δ^2 dependence.

It is observed that the average lattice spacing of the alloys closely follows Vegard's law

$$d_o = xa + (1-x)b\,. \tag{5}$$

Since the difference between the lattice parameters a and b of the binary compounds corresponds to the different AC and BC bond lengths, the bonds must be distorted or rearranged to form the alloy. If a and b do not differ too widely, the energy of the rearranged configuration must be of second order in $a - d_o$ and $b - d_o$. Thus the contribution to the enthalpy of formation

of the alloy is

$$\Delta H_m = \frac{\lambda}{\bar{d}^2} \left(x(d_o - a)^2 + (1 - x)(d_o - b)^2\right) \tag{6}$$

where λ is an adjustable parameter. With d_o from Equation (5) this becomes

$$\Delta H_m = x(1 - x)\lambda \left(\frac{\Delta}{\bar{d}}\right)^2 \tag{7}$$

with the same Δ^2 dependence as the DLP model.

Since we are viewing the effect as an elastic distortion, we can obtain a crude numerical estimate for λ from the macroscopic elastic properties of the crystal. At one extreme one can assume a strict virtual crystal model of the alloy, which would identify the bond distortion energy with that of an isotropic compression or dilatation. At x = 1/2, the principal strains are given by $1/2\Delta$ and the elastic energy per unit volume is

$$W = 1/2B \left(\frac{3}{2} \frac{\Delta}{\bar{d}}\right)^2 \tag{8}$$

yielding

$$\lambda = \frac{9}{2} BV, \quad \Omega' = \lambda \left(\frac{\Delta}{\bar{d}}\right)^2 \tag{9}$$

where B is the bulk modulus and V is the molar volume of the alloy with x = 1/2. Table 2.1 lists Ω_s and Ω' for the ternary compounds under discussion.

Equation (9), which contains no adjustable parameters, yields higher interaction parameter values than the DLP theory. A much better fit to the experimental data is obtained if the

prediction of Equation (9) is reduced by a factor of about 4.4, resulting in the column labeled Ω'' in Table 2.1. Indeed, the entries in that column fit the observed values as closely as Stringfellow's[2] "best fit" 2.45 power law. Moreover, a plausible case can be argued for a reduction of the estimate by a factor of this order.

It has been demonstrated recently[4] that although the average lattice parameter closely follows Vegard's law, the AC and BC bond lengths do not take the common nearest neighbor value of the virtual crystal but remain much closer, by a factor of 4 or 5, to their lengths in the binary compounds. If it is assumed that the stretching and compression of nearest neighbor bonds is the only distortion, this reduces the estimate of λ by the square of this factor, of order 20. This, however, almost certainly underestimates the effect of the distortion, since the conservation of nearest neighbor bond lengths requires a distortion of the bond angles and of second neighbor bond lengths and angles.

In addition, the fact that the AC and BC bond lengths tend to remain constant (to about 80%) independent of alloy composition, necessarily implies that the A and B atoms in the alloy are much more correlated than in a random solution. These strong correlations could well be due to the strong elastic forces. Neither our theory nor any other theory currently takes this into account properly. Thus within the scope of our model,

Table 2.1 Experimental and calculated values of the interaction parameter. Bulk moduli by interpolation between binary compound values from References 8 and 9; interaction parameters (in k cal/mole) in Columns 3, 4, and 5 quoted from Stringfellow, Reference 2 (small differences in the calculated values in Column 4 because we use fewer significant numbers than Reference 2 for $\Delta/\bar{d}$).

Alloy	$\frac{\Delta}{\bar{d}}$	$B \times 10^{-11}$ dyne cm^{-2}	Ω exp	Ω calc DLP	$1.74 \times 10^{6} (\Delta/\bar{d})^{2.45}$	Ω'	$\Omega'' = 0.226\Omega'$
AlGaP	0.002	8.73				0	0
AlInP	0.072	7.93				12100	2740
GaInP	0.074	8.05	3500,3250	3630	2940	13000	2940
AlGaAs	0.002	7.60	0	0	0	0	0
AlInAs	0.068	6.81	2500	2814	2370	10500	2370
GaInAs	0.070	6.67	1650, 3000,2000	2815	2510	10700	2420
AlGaSb	0.008	5.79	0	23	8	140	30
AlInSb	0.054	5.34	600	1456	1400	6400	1450
GaInSb	0.062	5.21	1475, 1900	1846	1830	8100	1830
AlPAs	0.036	8.17				3000	680
AlPSb	0.117	7.26				31600	7140
AlAsSb	0.081	6.83				15300	3460
GaPAs	0.036	8.16	400, 1000	985	446	2900	660
GaPSb	0.104	7.25				21300	4810
GaAsSb	0.075	6.[illegible]	4500, 4000	3355	3090	12200	2760
InPAs	0.032	6.57	400	585	436	2300	520
InPSb	0.099	6.01				22600	5110
InAsSb	0.067	5.32	2900, 2250	2289	2330	9600	2170

Table 2.1 furnishes strong evidence that this quasi-elastic energy is a significant, and perhaps a dominant part of the enthalpy of mixing.

2.2 COMPOSITION FLUCTUATIONS

A binary mixture whose enthalpy of mixing is positive has a tendency to separate into its components. This tendency manifests itself in the form of spinodal decomposition and the development of a miscibility gap below a critical mixing temperature and in the form of clustering on a microscopic scale above this temperature. In the alloys under discussion here, this tendency is most readily interpreted in terms of preferential pairwise interactions as expressed by Equations (2) and (3), but it does not depend on this interpretation. Jones, Porod, and Ferry[5] have recently examined the degree of clustering that may be expected to occur above the critical temperature of mixing as a function of the interaction parameter interpreted in this manner, of the temperature, and of the mole fraction x. We extend this calculation to include an elastic energy which is large enough to overcome the clustering tendency.

Since the lattice parameters of the alloys follow Vegard's law, the ions of the alloy at least on the average occupy positions on a virtual crystal lattice with the lattice parameter of Equation (5). Note that this statement is not in conflict with the observation cited above[4] that the bond lengths need not follow Vegard's law.

Clustering produces a fluctuation from the average composition, while the region of the cluster must occupy the volume prescribed by the average virtual crystal lattice. Thus the region of the cluster is strained. The energy associated with the strain tends to reduce the degree of clustering, but we shall see that it does not eliminate a miscibility gap below the critical mixing temperature. The effect is similar to the "lattice latching"[6] and stabilization against decomposition[7] associated with the mismatch strains of heteroepitaxy. In the present instance we deal with the strains arising from fluctuations in a homogeneous medium. In either case, the existence of a strained region presupposes the existence of a crystal lattice to be matched by the continuing growth. In epitaxy, this lattice is furnished by the substrate. In homogeneous growth it depends on the formation of a nucleus, which at a given composition can only form at temperatures above the spinodal decomposition curve. This is the reason why the strain energy affects clustering but not the miscibility gap.

Let the average composition of an alloy be $A_{x_o}B_{1-x_o}C$ and the local composition $A_xB_{1-x}C$. Then the lattice parameter is

$$d_o = x_o a + (1 - x_o)b. \tag{10}$$

If the crystal were permitted to relax everywhere, the local lattice parameter would be

$$d = xa + (1 - x)b. \tag{11}$$

However, the compatibility constraint imposes a local strain

$$\delta = d - d_o = (x - x_o)(a - b) \equiv \xi \Delta , \qquad (12)$$

the second equality defining the composition fluctuation ξ.

The energy density of the strain can be computed as in Equation (8) and is

$$W = (9/2) B \xi^2 \left(\frac{\Delta}{\bar{d}}\right)^2 \qquad (13)$$

per unit volume.

Unlike Equation (8) for the elastic contribution to the mixing enthalpy, Equation (12) should not be a significant overestimate of the strain energy. In the present application we are computing the energy of actual compressions and dilatations in terms of measured elastic constants and the nature of the bond distortions accompanying the strain is irrelevant. Therefore, if the mixing enthalpy is dominated by the bond distortion effects discussed in the last section, then it is evident that the strain energy of composition fluctuations is more than adequate to overcome the clustering tendency.

A similar argument can be made if the clustering is ascribed to preferential pairwise interactions. The molar bond energy density of the ternary alloy, taking into account the 4 nearest and 12 next nearest neighbor interactions is

$$E = N_o(4\varepsilon_A x + 4\varepsilon_B(1 - x) + 6\varepsilon_{AA}x^2 + 12\varepsilon_{AB}x(1 - x) + 6\varepsilon_{BB}(1 - x)^2), \qquad (14)$$

where ε_A and ε_B are the AC and BC interaction energies.

The contribution to the bond energy density of a composition fluctuation ξ is $E(x_o + \xi) - E(x_o) = \eta$, given by

$$\eta = N_o((4\varepsilon_A - 4\varepsilon_B + 12\varepsilon_{AB} - 12\varepsilon_{BB} - 12\, x_o\, \varepsilon)\xi - 6\varepsilon\xi^2) \tag{15}$$

with ε as defined in Equation (3).

In a crystal of a given composition, the contribution to the interaction energy linear in the fluctuations must by definition average to zero. Therefore only the term in ξ^2 need be considered for the purpose of minimizing the free energy. But from Equation (2) this term is just

$$\eta = -\Omega\xi^2, \tag{16}$$

so that the net molar energy of the fluctuations, from Equations (13) and (16), is

$$WV + \eta = (\Omega' - \Omega)\xi^2 \tag{17}$$

averaged over the crystal.

Equation (17) yields a positive (or zero) fluctuation energy for each of the ternary alloys we are considering, indicating that clustering is suppressed by the strain energy.

2.3 CONCLUSIONS

In our model the formation of a tetrahedral semiconductor alloy is accompanied by bond distortion, and an estimate of the electronic energy of this distortion can be obtained from the macroscopic elastic properties of the crystal. Superficially this view appears distinct from the basis of the DLP model, which is deduced from the empirical lattice parameter dependence

of the optical bandgap and from Van Vechten's proposal. But the bandgap itself, as pointed out by Phillips and Van Vechten[1], is a measure of the covalent bonding energy. The elastic constants of a crystal depend as directly on the bonding energy as its optical and dielectric properties. Therefore it is perhaps not too surprising that models derived from optical and from elastic crystal parameters should yield predictions of similar form for the thermodynamic properties. The merit we may claim for the elastic model is that it contributes a new and convenient experimental approach to the thermodynamic quantities and that it may yield useful theoretical insights.

2.4 REFERENCES

1. J.C. Phillips and J.A. Van Vechten, Phys. Rev. B2, 2147 (1970).
2. G.B. Stringfellow, J. Phys. Chem. Solids 34, 1749 (1973); J. Crystal Growth 27, 21 (1974).
3. J.A. Van Vechten, Handbook on Semiconductors, Vol. 3, S.P. Keller editor, (North-Holland, Amsterdam, 1980), Ch. 1, Sec. 3, pg. 52.
4. J. Mikkelsen, Jr. and J.B. Boyce, Phys. Rev. Lett. 49, 1412 (1982).
5. K.A. Jones, W. Porod, and D.K. Ferry, J. Phys. Chem. Solids 44, 107 (1983).
6. G.B. Stringfellow, J. Appl. Phys. 43, 3455 (1972).
7. G.B. Stringfellow, J. Appl. Phys. 54, 404 (1983).
8. G. Martinez, in M. Balkanski, ed., Handbook on Semiconductors v. 2,(North-Holland, Amsterdam, 1980).
9. J.D. Wiley, in R.K. Willardson and A.C. Beer, eds., Semiconductors and Semimetals v. 10, Academic Press, New York, (1975).

3. COMPOSITION CORRELATIONS IN ALLOYS

Ternary tetrahedrally coordinated semiconductor alloys $A_xB_{1-x}C$ or AC_xD_{1-x} where A and B are group III (or II) elements and C and D group V (or VI) elements can for many purposes be described as binary mixtures whose component particles reside (approximately) on the sites of an fcc lattice. Specifically, thermodynamic parameters such as mixing enthalpy[1] and spinodal curves[2] conform fairly well to the rules describing regular solutions.

The key quantity of regular solution theory is the interaction parameter Ω, which can be interpreted in terms of pair interaction energies, thus

$$\Omega = \frac{1}{2} N_o Z (2E_{AB} - E_{AA} - E_{BB}),$$

where N_o is Avogadro's number, Z is the coordination number (12 for fcc) and E_{ij} are the (negative) pair interaction energies. A negative value of Ω indicates a tendency to ordering (compound formation), a positive value a tendency to decomposition. All the observed interaction parameters of the alloy group with A = Al, Ga, In; B = P, As, Sb; A = Zn, Cd, Hg; B = Se, Te are positive or zero. Thus one expects - and observes - miscibility gaps and spinodal decomposition below a critical mixing temperature characteristic of each alloy.

The observed interaction parameters are found to be proportional to the square of the lattice parameter difference between the pure compounds that constitute the alloy. This

dependence has been interpreted, in the so-called delta-lattice-parameter (DLP) model in terms of the lattice parameter dependence of the average bandgap[3], and more recently, especially after details of the composition dependence of bond lengths in $Ga_{1-x}In_xAs$ were revealed by EXAFS measurements[4], in terms of the bond distortions associated with the formation of the alloy. By relating the bond distortion energies to the macroscopic elastic constants of the crystals, a good case could be made for ascribing most or all of the observed mixing enthalpy to this cause[5],[6].

A positive mixing enthalpy would normally produce clustering of like particles above the critical mixing temperature, and an estimate of the degree of clustering to be expected was published recently[7]. For the model that was used in this calculation, the origin of the positive interaction parameter is irrelevant. It has been pointed out, however, that in the type of "lattice gas" that represents these alloys, with a composition dependent lattice parameter, if an alloy crystal is formed at all, elastic interactions will suppress the clustering[5]. It was also suggested that these elastic interactions were likely to produce an ordering tendency, that is to say, that local composition fluctuations might be reduced below the level to be expected of a purely random distribution of the constituents. What follows is a simple thermodynamic model for the composition correlations induced by the elastic energy.

3.1 THERMODYNAMIC MODEL

The lattice parameters of these alloys follow Vegard's law quite accurately. Any deviation from a linear dependence of lattice parameter on composition (bowing) is small enough to be quite negligible for the purpose of this argument. Consider a region of the alloy large enough to be regarded as macroscopic. If the composition of this region deviates from the average composition of the alloy, but must be accomodated in the volume of the virtual lattice that "belongs to it", it will suffer compression or dilatation. This is illustrated schematically in Figure 3.1.

The energy associated with this strain is readily computed[5]. Let the average composition of the alloy be $A_{x_o}B_{1-x_o}C$ and the local composition $A_xB_{1-x}C$. Then the lattice parameter is

$$d_o = x_o\, a + (1-x_o)b \tag{1}$$

where a is the lattice parameter of AC and b the lattice parameter of BC. If the crystal were permitted to relax everywhere, the local lattice parameter would be

$$d = xa + (1-x)b, \tag{2}$$

however, the compatibility constraint imposes a local strain

$$\delta = d-d_o = (x-x_o)(a-b) \equiv \Delta x\ (a-b) \tag{3}$$

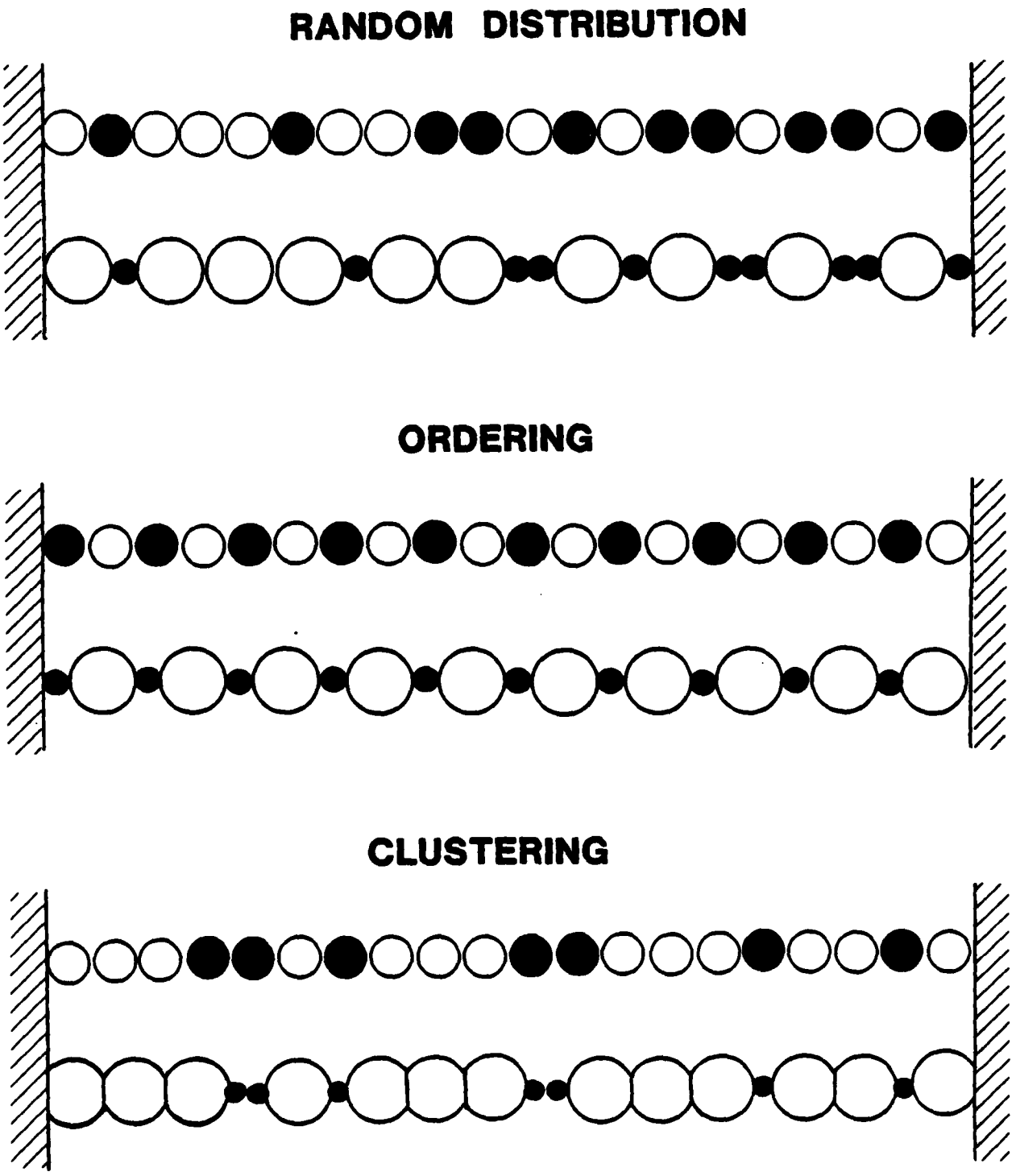

Figure 3.1 Schematic illustration of the effects of nonrandom distribution of atoms in III-V alloys with like-sized and different-sized atoms.

with an associated energy density (per unit volume)

$$W(\Delta x)^2 = 18B \left(\frac{a-b}{a+b}\right)^2 (\Delta x)^2 \qquad (4)$$

where B is the bulk modulus of the crystal.

Equation (4) is based on isotropic compression or dilation; an analogous expression can be obtained for a planar strain. In that form the elastic energy is thought to be responsible for the "lattice latching" observed in heteroepitaxy[8], the growth of a single lattice-matched alloy composition over a range of melt compositions. It also accounts for the successful heteroepitaxial growth of alloy compositions unstable in the bulk at the growth temperature.

It has been shown[5] that a reasonable fit to the interaction parameters of the III-V alloys considered here is given by the semi-empirical formula

$$W' = 0.226 \times 18B \left(\frac{a-b}{a+b}\right)^2 \qquad (5)$$

making a contribution the the mixing enthalpy per mole of

$$\Delta H = W'x(1-x)V \qquad (6)$$

where V is the molar volume of the alloy.

The entropy of mixing is approximately

$$S = \ln \frac{N_A!\ N_B!}{N_{AA}!\ N_{BB}!\ (N_{AB}!)^2} \qquad (7)$$

where the N_i are numbers of ions and the N_{ij} numbers of second neighbor pairs. Per mole this is

$$S \approx R[x\ln x + (1-x)\ln(1-x) - x^2\ln(x^2) - (1-x)^2\ln(1-x)^2 - 2x(1-x)\ln x(1-x)]. \quad (8)$$

Using Equations (4), (6), and (8) in the thermodynamic formula[9] for macroscopic fluctuations of concentration on an assembly of N sites with total Gibbs free energy G

$$\langle(\Delta x)^2\rangle = \frac{kT}{(\partial^2 G/\partial x^2)_{T,P,N}} \quad (9)$$

we find

$$\langle(\Delta x)^2\rangle = \frac{1}{N} x(1-x)\left[1 + \frac{2(W-W')V}{RT} x(1-x)\right]^{-1} \quad (10a)$$

or, in terms of the critical mixing temperature T_c given by $2RT_c = W'V = 0.226WV$

$$\langle(\Delta x)^2\rangle = \frac{1}{N}\left[\frac{x(1-x)}{1 + 13.7\frac{T_c}{T}x(1-x)}\right] \quad (10b)$$

One may guess conservatively that the disorder grown into a crystal corresponds roughly to a value frozen in at the growth temperature. Thus if we compare a lattice-matched alloy such as $Ga_{0.5}Al_{0.5}As$ with $T_c \approx 0$ with the mismatched alloy $In_{0.5}Ga_{0.5}As$ with $T_c \sim 600^\circ K$ grown epitaxially at $T \sim 900^\circ K$, we expect, from Equation (10a) or (10b) to find a relative reduction of the mean square concentration

fluctuations in the mismatched alloy by a factor of ~ 0.3. The reduction would be expected to be more significant, depending on cooling rate and on other growth parameters, if appreciable solid state diffusion takes place after growth.

3.2 RAMAN SCATTERING ANALYSIS

Some qualitative experimental support for this prediction is to be found in linewidths and lineshapes observed by Parayanthal and Pollak[10] in Raman scattering from $Al_xGa_{1-x}As$ and $In_xGa_{1-x}As$. In this work it was found that the broadening and asymmetry of the Raman line was more pronounced in the lattice-matched alloy $Al_xGa_{1-x}As$ than in the mismatched $In_xGa_{1-x}As$.

A "spatial correlation" model has been successfully used to interpret the effect of microcrystalline[11], and implantation damage[12] disorder on Raman linewidths and lineshapes. This model replaces the phonons of the infinite ordered crystal with phonons localized within "correlation regions" whose size is a measure of the partial ordering in the imperfect crystal. As a result, the $q = 0$ momentum selection rule of the perfect crystal is relaxed, and phonons in a region of the Brillouin zone corresponding to the correlation length participate in the scattering. Experimental values of the correlation length are deduced by fitting the observed linewidths and lineshapes, assuming a gaussian size distribution of the correlation regions, generally in reasonable agreement with the estimated sizes of crystallites[11] or undamaged regions[12].

Substitutional disorder in an alloy similarly breaks the crystal's translational symmetry and hence the $q = 0$ selection rule for Raman scattering. Since the perturbation is the phonon modulation of the dielectric tensor, the effective size of the scattering regions is given by the correlation length of this tensor's spatial fluctuations[13]. No theoretical prediction has so far been made for this quantity, but Parayanthal and Pollak[10] were able to fit their observed Raman lines with a spatial correlation model in which the correlation length is simply a phenomenological parameter determined from the experimental data. For their epitaxially grown alloys, this parameter ranges from about 8 to above 30 lattice parameters.

Of the two alloy series for which results are given, $Ga_xAl_{1-x}As$ has, within experimental accuracy, zero mixing enthalpy, and the cations should constitute a perfect lattice gas on their fcc sublattice. Their concentration fluctuations, which may be taken as a measure of the disorder, then are given by Equations (10) with $T_c = 0$. The Raman lines bear this out qualitatively, in the sense that the linewidths and asymmetries are greatest for samples with x near 0.5.

The broadening of the Raman lines even in the completely random alloy $Ga_xAl_{1-x}As$ is modest as compared with the spectrum of amorphous materials, and the spatial correlation model is successful in the interpretation of the lineshapes. This suggests that one might assign the role of the defects

that disrupt the phonon modes to fairly large fluctuations from the average composition. The correlation or coherence length can then be related to the statistics of large fluctuations.

In a random binary alloy, the probability distribution of ions is binomial. With a coordination number $Z = 12$, the distribution of even the nearest neighbor shell is fairly well represented by a Gaussian, and the probability of occurrence of a deviation $\geq \xi$ is approximated by

$$P(\xi) = \text{erfc } \zeta \tag{11}$$

where $\zeta \equiv \xi/\sqrt{2 <(\Delta x)^2>}$.

In order to arrive at an order of magnitude estimate of the correlation length, we take the size of the defect to comprise one cation shell of Z ions. If a deviation of relative magnitude ξ is to occur in a region containing NZ cations, we should have $NZP(\xi) = 1$, and therefore the average distance between such defects, which we take to be the correlation length, is

$$L = N^{1/3}a = (Z \text{ erfc } \xi)^{-1/3}a \tag{12}$$

where a is the lattice parameter. Equation (12) yields values consistent with the estimates based on the Raman spectra if ξ is about two standard deviations. Using the average value of L for the GaAs-like mode in $Ga_xAl_{1-x}As$ for the four samples with x near 0.5, we find $\xi = 1.88$.

Equations (10) and (12) also provide a comparison of the correlation lengths in $Ga_xIn_{1-x}As$ and $Ga_xAl_{1-x}As$. Because of the suppression of concentration fluctuations, we expect the scattering centers associated with wide fluctuations to be rarer, increasing the correlation length. Using the factor 0.3 estimated from Equation (10) for the reduction in the mean square fluctuation in Equation (12), we find

$$\frac{L_{Ga_{0.5}In_{0.5}As}}{L_{Ga_{0.5}Al_{0.5}As}} \approx 12. \qquad (13)$$

This factor is larger than the numbers deduced from the Raman spectra by Parayanthal and Pollak, suggesting that additional phonon scattering processes are active.

3.3 X-RAY LAUE PATTERNS

The reduction in randomness discussed above is expected to have other experimentally testable consequences. For example, it is possible to examine such effects with x-ray back-reflection Laue photographs, where long-range order in a III-V alloy would produce reflections other than those expected for the sphalerite crystal structure. Figure 3.2(a) shows a Laue pattern for an $Al_{0.4}Ga_{0.6}As$ epitaxial layer grown on a GaAs substrate, while Figure 3.2(b) shows a pattern with the same crystal orientation for an $In_{0.5}Ga_{0.5}P$ epitaxial layer. No additional spots are observed for the $In_{0.5}Ga_{0.5}P$ over the $Al_{0.4}Ga_{0.6}As$, indicating no long-range order. The 064 and $0\bar{6}4$ reflections, however, are much more intense for $In_{0.5}Ga_{0.5}P$ than for $Al_{0.5}Ga_{0.5}As$. We are currently examining the implications of these measurements for correlations and ordering in these alloys.

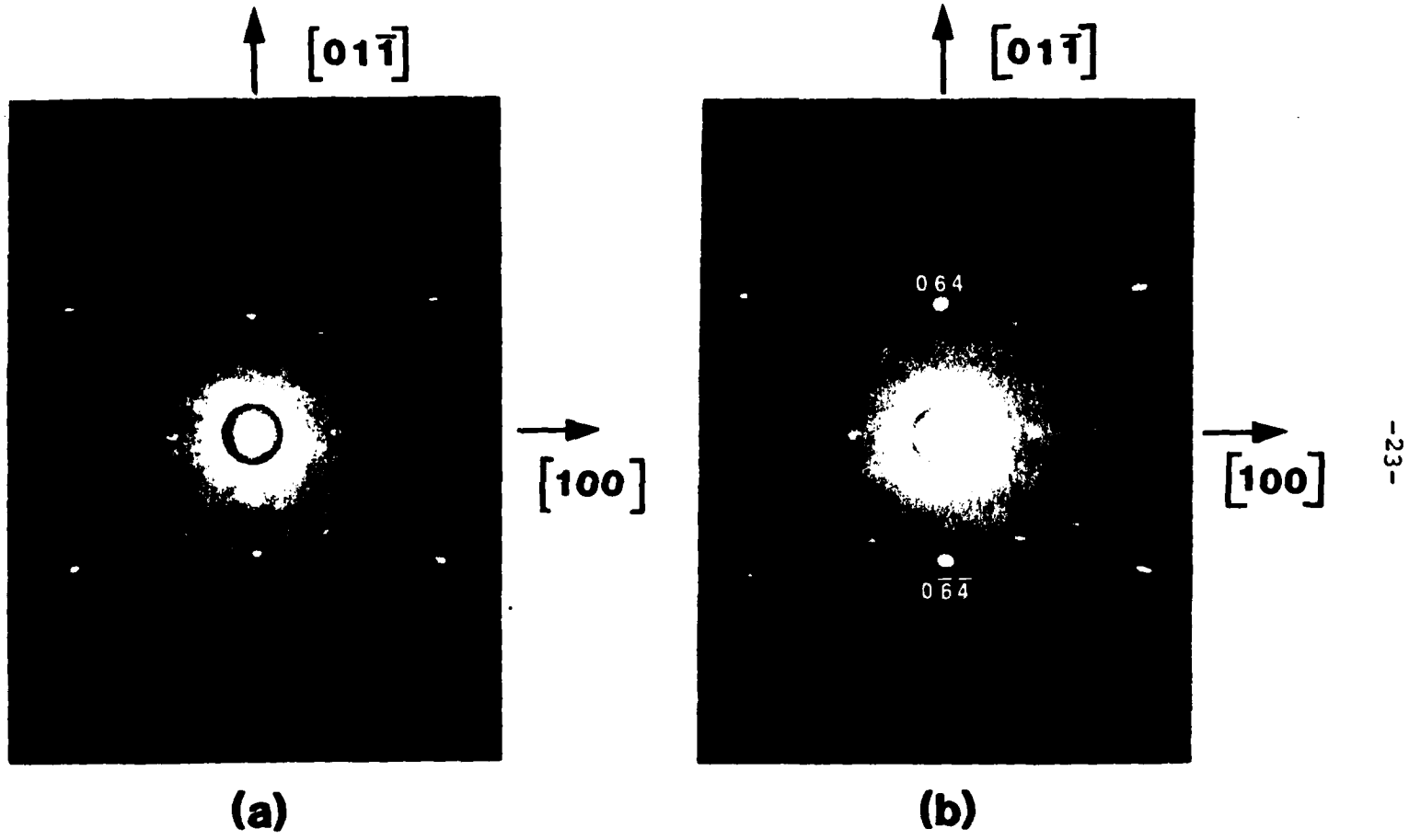

Figure 3.2 Back-reflection Laue photographs for (a) an $Al_{0.4}Ga_{0.6}As$ epitaxial layer and (b) an $In_{0.5}Ga_{0.5}P$ epitaxial layer, both grown on GaAs substrates.

3.4 REFERENCES

1. G.B. Stringfellow, J. Phys. Chem Solids 33, 665 (1972).
2. G.B. Stringfellow, J. Appl. Phys. 54, 404 (1983).
3. G.B. Stringfellow, J. Cryst. Growth 27, 21 (1974); J.C. Phillips and J.A. VanVechten, Phys. Rev. B2, 2147 (1970).
4. J.C. Mikkelsen, Jr. and J.B. Boyce, Phys. Rev. Lett. 49, 1412 (1982).
5. P.A. Fedders and M.W. Muller, J. Phys. Chem. Solids, to be published.
6. J.C. Mikkelsen, Jr., private communication.
7. K.A. Jones, W. Porod, and D.K. Ferry, J. Phys. Chem. Solids 44, 107 (1983).
8. G.B. Stringfellow, J. Appl. Phys. 43, 3455 (1972).
9. A. Münster, in "Fluctuation Phenomena in Solids", R.E. Burgess, ed., Academic Press, New York 1965, p 184.
10. P. Parayanthal and F.H. Pollak, Phys. Rev. Lett. 52, 1822 (1984).
11. H. Richter, Z.P. Wang, and L. Ley, Solid St. Com. 39, 625 (1981).
12. K.K. Tiong, P.M. Amirtharay, F.H. Pollak and D.E. Aspnes, Appl. Phys. Lett. 44, 122 (1984).
13. R. Shuker and R.W. Gammon, Phys. Rev. Lett. 25, 222 (1970).

4. BELOW BANDGAP PHOTORESPONSE IN $In_{1-x}Ga_xP$-GaAs HETEROJUNCTIONS

Several schemes have been used in intrinsic infrared photodetectors to obtain response below the bandgap of the constituent semiconductors. One of these methods is to form an alloy between two compounds which have conduction and valence bands of opposite symmetry, such as PbTe and SnTe[1]. Since the conduction and valence bands must interchange at some alloy composition, they move toward one another producing alloy bandgaps smaller than the endpoints. Another method uses electroabsorption (photon-assisted tunneling) to shift the absorption edge to longer wavelengths[2]. This has been employed in reverse-biased GaAs[3] and $Ga_{1-x}Al_xAs$ devices[4]. A recently proposed scheme is to form an alloy between two materials with different crystal structures. In the region where the alloy undergoes a phase change from one structure to another, the absorption edge is lowered due to antisite disorder. This behavior has been observed in $(GaAs)_{1-x}Ge_{2x}$ alloys[5]. In the present work we discuss and present experimental evidence for what appears to be another method of obtaining longer wavelength response.

The scheme is essentially the inverse of a photon emission process previously described[6]. It employs the electric field at the interface of a heterojunction to tunnel charge carriers across an interfacial energy gap smaller than the energy gaps of the semiconductors on either side. Photoresponse is obtained by the photoexcitation of electrons from the valence band of one material to virtual states,

and then electron tunneling into the conduction band of the other material. Conversely, electtons from the valence band of one material can tunnel into virtual states and then be photo-excited into the conduction band of the other material. The latter process is equivalent to hole tunneling, and both are illustrated schematically in Figure 4.1.

4.1 ABRUPT HETEROJUNCTION MODEL

One of the heterojunction systems which exhibits the required energy band line-up is $In_{1-x}Ga_xP$-GaAs. An abrupt heterojunction model for this system is shown in Figure 4.1. Several of the parameters of the model vary from sample-to-sample and were determined in the following ways: The energy gap of GaAs was measured by photoconductivity on high-purity epitaxial samples to be 1.39eV. The energy gap of $In_{1-x}Ga_xP$ was determined from its dependence on lattice constant[7], where the latter was obtained by double-crystal X-ray diffraction scans. On this basis the energy gap of the lattice-matched alloy $In_{0.49}Ga_{0.51}P$ was 1.90eV. The separations between the electrochemical potential energy, ζ, and the band edges were determined from Hall measurements: first on the GaAs substrates and then on $In_{1-x}Ga_xP$ layers grown on semi-insulating GaAs by liquid phase epitaxy under the same conditions as those grown on n^+ substrates. The built-in potential and the band-bending on either side were obtained from capacitance-voltage measurements. From these measurements all the parameters of the model, including $\Delta\mathcal{E}_V$, $\Delta\mathcal{E}_C$, and $\Delta\mathcal{E}_I$, were determined experimentally.

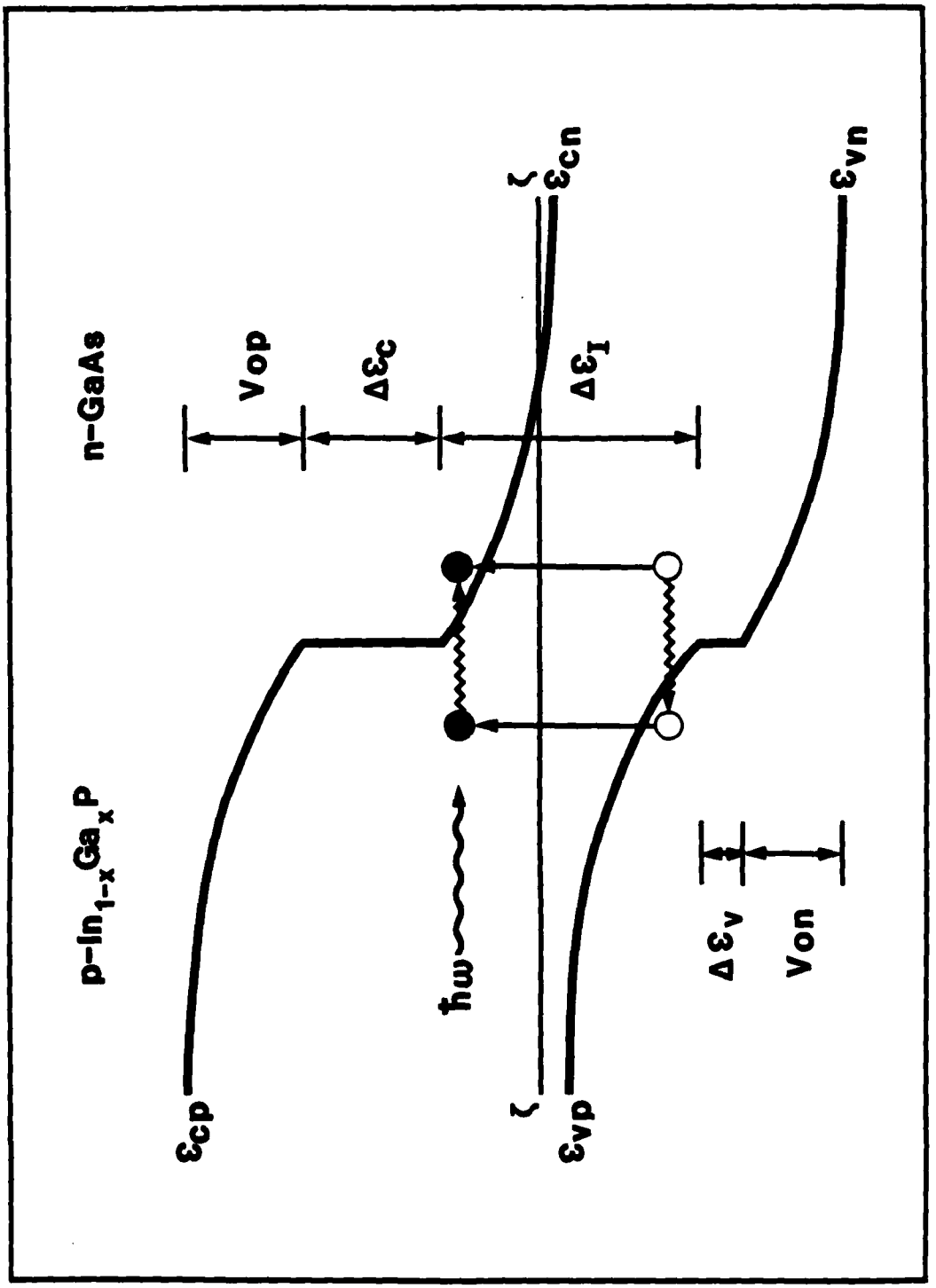

Figure 4.1 Abrupt heterojunction model for $In_{1-x}Ga_xP$-GaAs indicating schematically the photon-assisted tunneling processes for electrons on the p-side and holes on the n-side.

For a lattice-matched heterojunction with a nominal {111} interface, the band offsets were $\Delta\mathcal{E}_V = 0.08$eV, $\Delta\mathcal{E}_C = 0.59$eV, and $\Delta\mathcal{E}_I = 1.31$eV. Although these results are consistently obtained experimentally, it should be pointed out that they are not close to the expected theoretical values. Using a dielectric model[8], for example, we calculate ionization energies for GaAs and $In_{0.49}Ga_{0.51}P$ of 5.68eV and 5.91eV, respectively. These ionization energies and the experimental energy gaps yield band offsets of $\Delta\mathcal{E}_V = -0.23$eV, $\Delta\mathcal{E}_C = 0.28$eV, and $\Delta\mathcal{E}_I$ equals the bandgap of GaAs. Thus, below bandgap photoresponse is not predicted from this dielectric model. Although there is probably no reason to expect good agreement between theory and experiment, we have some preliminary evidence that the valence band offset is in the predicted direction for $In_{1-x}Ga_xP$-GaAs heterojunctions with nominally charge-neutral[9] {211} interfaces. Thus, at least part of the difference in band lineups may be due to dipoles associated with the residual charge at {111} interfaces.

4.2 PHOTOVOLTAIC RESPONSE

Figure 4.2 shows the room temperature photovoltaic response for a {111} heterojunction at 0 and -0.5 volt applied bias. (These diodes were rather leaky and exhibited substantially increased noise at higher reverse voltages). The salient features are a below-bandgap peak with a half power point at 1.31eV which increases substantially with reverse bias as expected for tunneling. The 1.31eV half-power point is equal to the value obtained for the interfacial

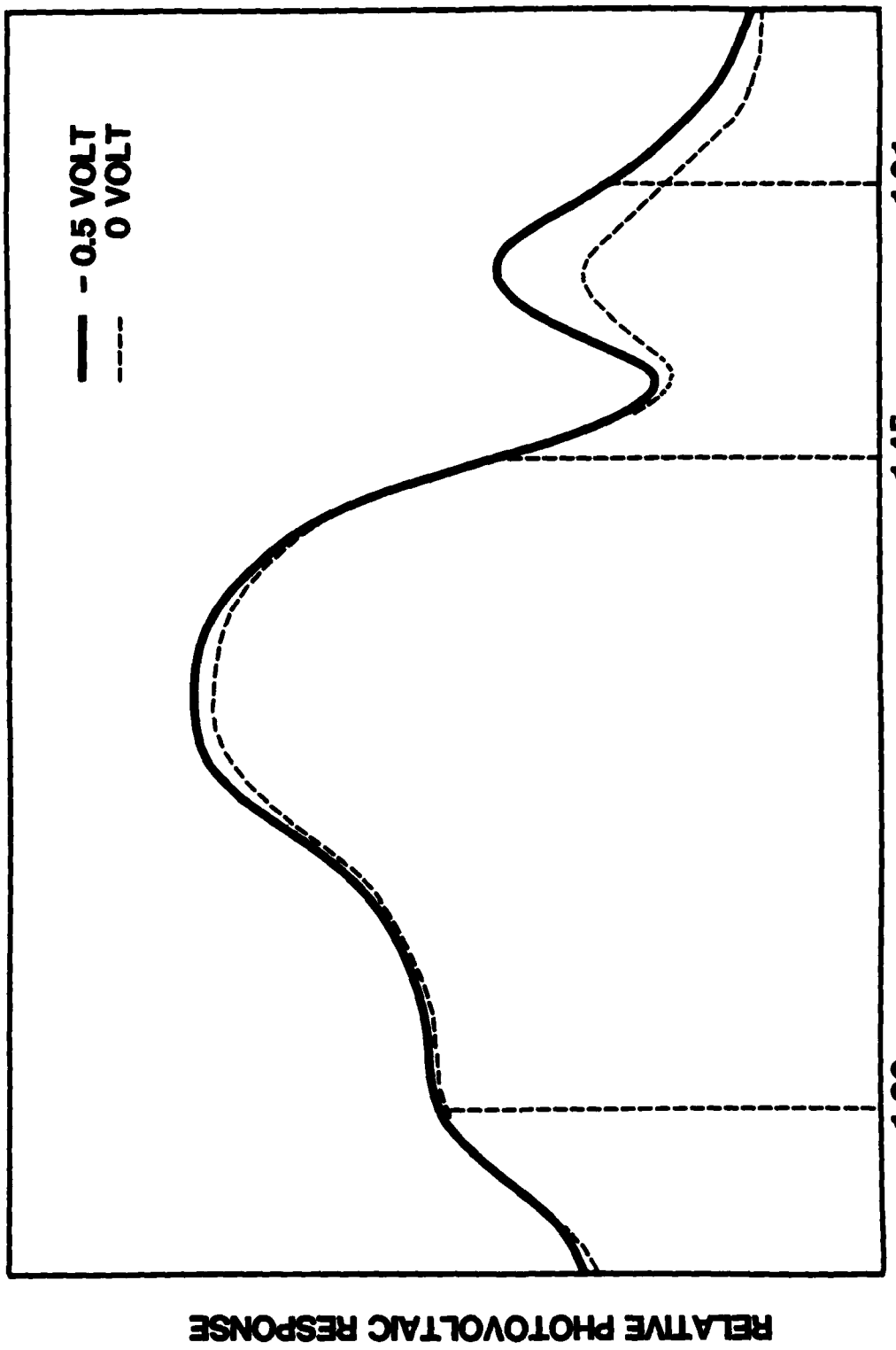

Figure 4.2 Relative photovoltaic response as a function of photon energy for the heterojunction of Figure 4.1 showing below bandgap response at two bias voltages.

energy gap, $\Delta\mathcal{E}_I$. This exact agreement, however, should not be taken seriously. Also, in this heterojunction the $In_{1-x}Ga_xP$ epitaxial layer was doped to produce $2.5 \times 10^{17} cm^{-3}$ holes, while the GaAs substrate had $1.4 \times 10^{18} cm^{-3}$ electrons. Thus, most of the potential was in the $In_{1-x}Ga_xP$ where it should enhance the lower-effective-mass and higher probability electron tunneling. The GaAs absorption edge is apparently shifted to higher than bandgap energy due to the high electron concentration[10].

To test the concept that the below-bandgap response is associated with tunneling across the interfacial energy gap, several other experiments were performed. When the doping of the p-type $In_{1-x}Ga_xP$ was increased from 2.5×10^{17} to $6.0 \times 10^{18} cm^{-3}$ on the same n-type GaAs substrates, the below-bandgap response was greatly reduced. Increased doping on the p-side is expected to reduce electron tunneling. Since larger-effective-mass hole tunneling from the n-side is much less probable, the smaller below-bandgap response is consistent with a tunneling mechanism. To eliminate the possibility that the below-bandgap response was due to impurity transitions in the space-charge region on either side of the interface, photoconductivity measurements were performed on the epitaxial layer and on the substrate. These measurements indicated no below-bandgap photoresponse. Except for the coincidence of the response energy with $\Delta\mathcal{E}_I$, we cannot,

however, rule out the possibility of impurity transitions at the interface itself.

4.3 CONCLUSIONS

In conclusion, we have observed below-bandgap photovoltaic response in $In_{1-x}Ga_xP$-GaAs p-n heterojunctions which is apparently due to photon-assisted tunneling across the interfacial energy gap between the two materials. Although the observed response for {111} interfaces at 1.31eV is not at a particularly useful wavelength, it should be possible to apply the same idea for infrared detectors at longer wavelengths. We are currently investigating the possibility of obtaining smaller interfacial energy gaps in the $In_{1-x}Ga_xP$-GaAs system by examining interfaces with different orientations. Other lattice-matched heterojunction systems, of course, should also be examined. Our results indicate, however, that heterojunctions with the required band lineups can not be predicted with great reliability.

4.4 REFERENCES

1. J.O. Dimmock, I. Melngailis, and A.J. Strauss, Phys. Rev. Lett. 16, 1193 (1966).
2. W. Franz, Z. Naturforsch, 13a, 484 (1958); L.V. Keldysh, Sov. Phys. JETP 7, 788 (1958).
3. G.E. Stillman, C.M. Wolfe, J.A. Rossi, and J.P. Donnelly, Appl. Phys. Lett. 11, 671 (1974).
4. J.C. Dyment, F.P. Kapron, and A.J. Springthorpe, Inst. Phys. Conf. Ser. No. 24 (Inst. Phys., London, 1975) p. 200.
5. Kathie E. Newman and John D. Dow, Phys. Rev. B 27, 7495 (1983).
6. H. Kroemer and G. Griffiths, IEEE Electron Device Lett. 4, 20 (1983).
7. G.B. Stringfellow, P.F. Lindquist, and R.A. Burmeister, J. Electron. Mat. 1, 437 (1972).
8. J.A. Van Vechten, Phys. Rev. 187, 1007 (1969).
9. W.A. Harrison, E.A. Kraut, J.R. Waldrop, and R.W. Grant, Phys. Rev. B 18, 4402 (1978).
10. E. Burstein, Phys. Rev. 93, 632 (1954); T.S. Moss, Proc. Phys. Soc. (London) B 76, 775 (1954).

5. BELOW BANDGAP EMISSION FROM $ZnSnP_2$-GaAs HETEROJUNCTIONS

Part of this program involves the use of the ordered chalcopyrite compound $ZnSnP_2$ as a template to obtain long-range order in the alloy $In_{0.5}Ga_{0.5}P$. The compound $ZnSnP_2$ lattice matches GaAs and these two materials, because of their different P and As anions, produce a heterojunction lineup with interesting potential applications[1].

Figure 5.1(a) shows the energy band diagram of a $ZnSnP_2$-GaAs heterojunction under forward bias. In this configuration electrons in the conduction band accumulation region can tunnel into the forbidden gap and recombine with holes in the valence band accumulation region (and vice versa). This should produce infrared emission below the bandgap of either material. Figure 5.1(b) shows the actual emission spectra from such a structure, indicating that such a scheme is feasible. The larger peak at higher energy is emission from the bandgap of GaAs, while the smaller peak at lower energy is apparently emission from the residual bandgap between GaAs and $ZnSnP_2$. We are currently investigating this process in more detail.

REFERENCE

1. H. Kroemer and G. Griffiths, IEEE Elect. Dev. Lett. 4, 20 (1983).

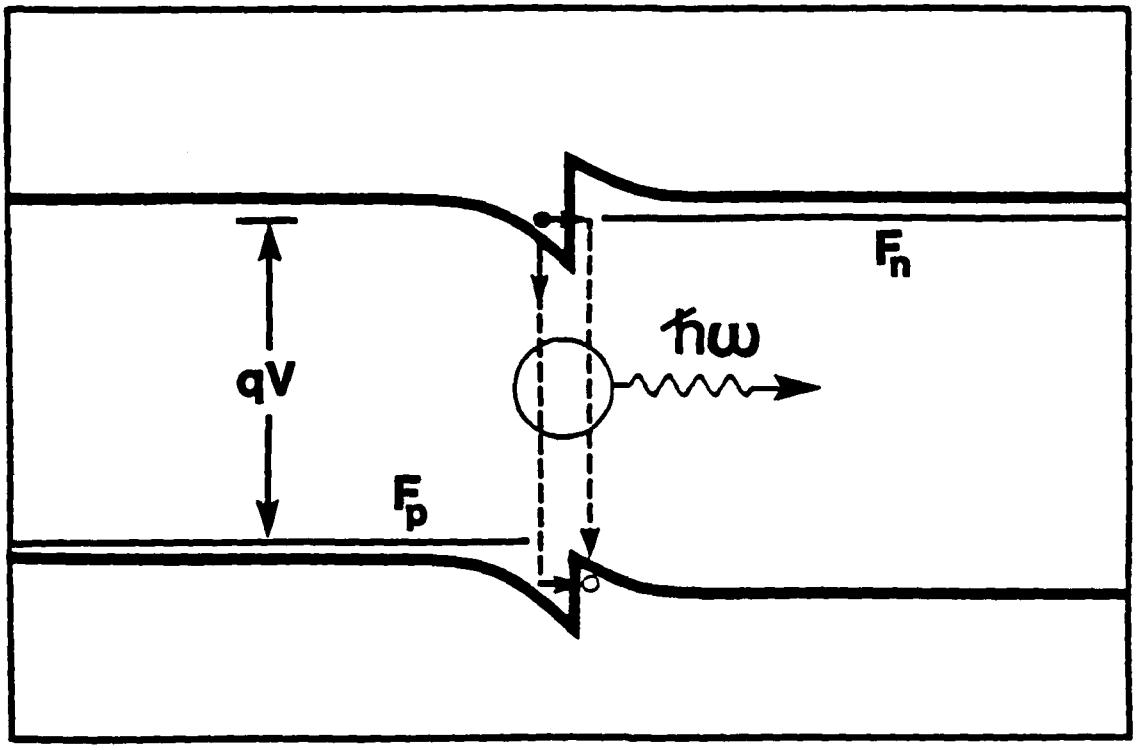

(a)

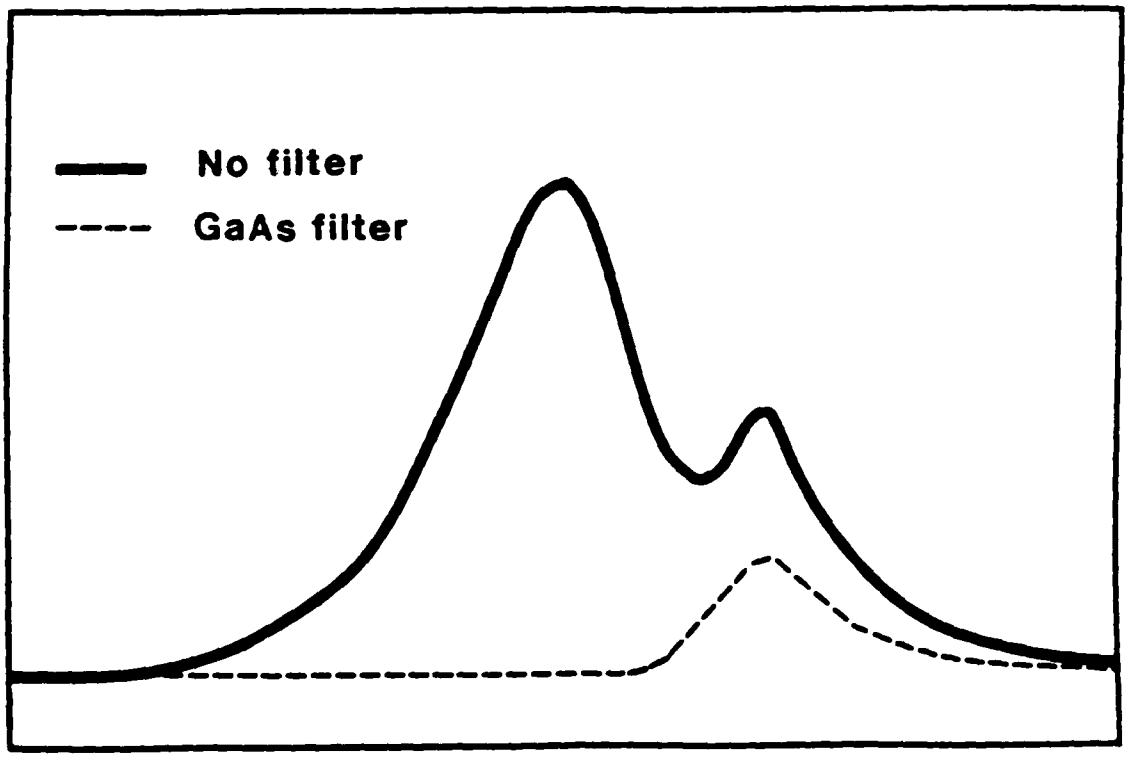

(b)

Figure 5.1 (a) Abrupt heterojunction model for $ZnSnP_2$-GaAs under forward bias. (b) Emission spectrum from structure in (a).

6. PUBLICATIONS

1. G.A. Davis and C.M. Wolfe, "Liquid Phase Epitaxial Growth of $ZnSnP_2$ on GaAs", J. Electrochem. Soc. 130, 1408 (1983).

2. G.A. Davis, M.W. Muller, and C.M. Wolfe, "Antiphase Domain Boundary Suppression in Chalcopyrite-on-Sphalerite Epitaxy", J. Crystal Growth (to be published).

3. P.A. Fedders and M.W. Muller, "Mixing Enthalpy and Composition Fluctuations in Ternary III-V Semiconductor Alloys", J. Phys. Chem. Solids (to be published).

4. M.W. Muller, "Composition Correlations in Ternary Semiconductor Alloys", submitted to Phys. Rev. Letters.

5. S. Julie Hsieh, Elizabeth A. Patten, and C.M. Wolfe, "Below Bandgap Photoresponse of $In_{1-x}Ga_xP$-GaAs Heterojunctions", submitted to Appl. Phys. Letters.

8. TALKS

1. M.W. Muller, "Mixing Enthalpy and Composition Fluctuations in Ternary III-V Semiconductor Alloys", Seminar, SRI International, Menlo Park, Calif., 20 December 1983.

END

FILMED

3-85

DTIC